Green Synthesis of Copper Nanoparticles Using *Centaurea cyanus* Plant Extract: A Cationic Dye Adsorption Application

Davarnejad, Reza*[+]

Department of Chemical Engineering, Faculty of Engineering, Arak University, Arak, I.R. IRAN

Azizi, Amir

Department of Chemistry, Faculty of Science, Arak University, Arak, I.R. IRAN

Asadi, Sajjad; Mohammadi, Maryam

Department of Chemical Engineering, Faculty of Engineering, Arak University, Arak, I.R. IRAN

ABSTRACT: *In this study, copper nanoparticles (Cu-NPs) were synthesized through green and economic techniques. The Centaurea cyanus plant extract was used as an appropriate reducing and stabilizing agent in this process. The synthesized nanoparticles were characterized by Fourier-Transform InfraRed (FT-IR) spectroscopy, X-Ray powder Diffraction (XRD), Field Emission Scanning Electron Microscopy (FESEM), Transmission Electron Microscopy (TEM), and N_2 adsorption porosimetry analysis. The analysis showed that the average size of spherical nanoparticles was around 11.9 nm, with 74.2 m^2/g and 0.36 cm^3/g mane surface area and pore size, respectively. Then, Cu-NPs were studied as a low-cost adsorbent to remove Methylene Blue (MB) dye from aqueous solutions. For this purpose, Central Composite Design (CCD) under the Response Surface Methodology (RSM) was applied to design the experiments, model the data, and optimize the operating conditions. The effect of various operating parameters such as pH, MB initial concentration, adsorbent amount, and contact time on the MB removal was practiced. Analysis of variance (ANOVA) showed a good agreement between the experimental data and the predicted ones obtained from the quadratic model. The optimum conditions for MB removal (63.20 %) were found at pH of 6.6, MB initial concentration of 30 mg/L, adsorbent amount of 0.15 g, and time of 101.5 min. The results showed that the Langmuir isotherm with a maximum adoption capacity of 21.9 mg/g and pseudo-second-order kinetic models with a rate constant of 0.359 (g/mg) (1/min) can properly legitimize the experimental data.*

KEYWORDS: *Green synthesis, Centaurea cyanus, Copper nanoparticles, Adsorption, Optimization*

INTRODUCTION

Copper nanoparticles (Cu-NPs) have been proposed as a suitable substitute for the expensive nanomaterials such as gold and silver to be used in the various industries such as medical, electronics, biotechnological and environmental ones [1]. There are various physical and chemical techniques for nanoparticle production [1-3].

To whom correspondence should be addressed.
+E-mail: R-Davarnejad@araku.ac.ir
1021-9986/2022/1/1-14 14/$/6.04

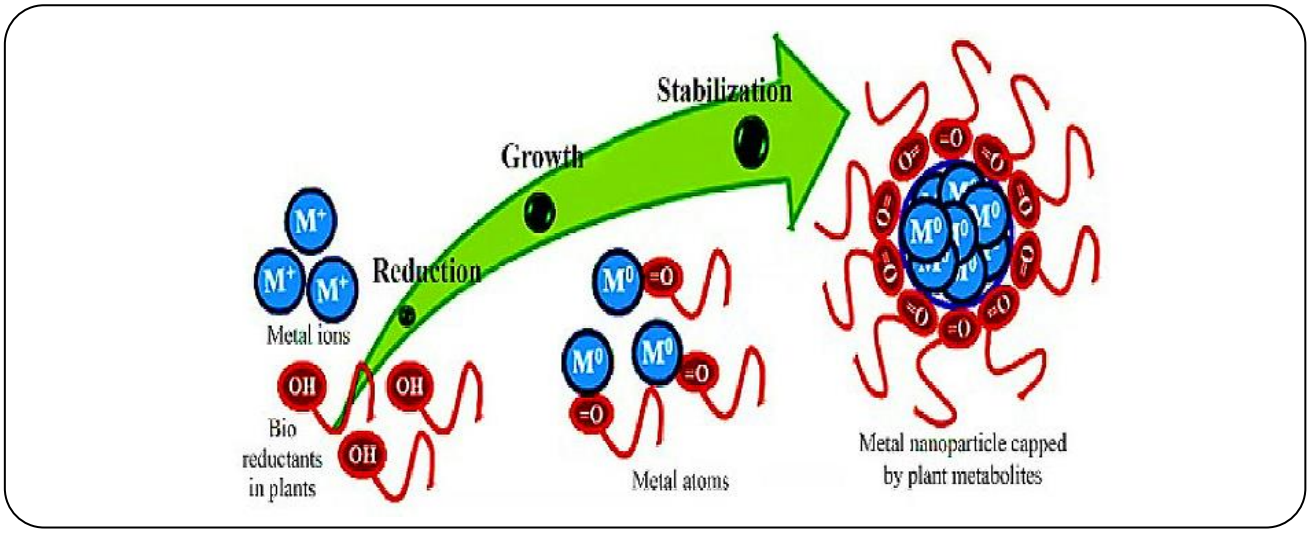

Fig. 1: Schematic mechanism of the green synthesis of metal nanoparticles production stages.

According to the environmental protocols, there are several limitations to toxic and hazardous chemicals. Therefore, some non-toxic, biological, and green methods are encouraged for this purpose [2-5]. The copper nanoparticles have widely been synthesized based on the recent techniques [6-8]. According to the literature, there are numerous reports on the herbal extracts which were used as the reducing and stabilizing agents. Fig. 1 briefly proposes a mechanism for the green synthesis of metal nanoparticles [9].

As Fig. 1 shows, the process involves three stages. In the first stage, the metal ions are transferred from their higher oxidation states to zero-valent metallic by acting plant metabolites (as green reducing agents), after nucleating the reduced metal atoms. In the second stage, metal atoms are collected to form metal nanoparticles while further biological reduction of metal ions occurred. The third stage in this method is the termination phase in nanoparticles. They finally found a stable morphology and were capped by plant metabolites. These steps have attributed to the reduction of metal ion oxidation states which leads to a change in the color of the solution media as the first indication of the synthesis of nanoparticles [10-14]. The reaction is fast and generally completed within a few minutes [15]. Optimization of this process is the main problem due to controlling nanoparticles' shape and size. It has usually been observed that temperature and pH control the reaction rate, growth process, and size of metal nanoparticles [16]. Some hypotheses have been proposed for the green synthesis of metal nanoparticles using plant extracts. However, the metal nanoparticles formation mechanism is not yet known but, it is still needed. The most acceptable mechanism is given in Fig. 2, which has also been reported by the other researchers. In this mechanism, the divalent copper ions [Cu(II) metal ion examined in this study] are reduced to zero-valent metallic copper Cu(0) or Cu-NPs by quercetin as a polyphenolic compound in the extract of some plants [9, 17].

In fact, electrons of functional groups (such as carbonyl from C ring in the Redox system) are able to transfer to the free orbital of copper ions and reduce them to zero metallic copper. The stabilization of the synthesis of copper particles is achieved via complexation with carbonyl (C=O) groups formed by the oxidation of hydroxide (OH) groups from the phenolic ring [9, 18, 19].

Since *Centaurea cyanus* plant is an agricultural waste that is abundantly found in Iran and a lot of countries, the polyphenolic compounds in its extract of it [such as flavonoids (e.g. anthocyaninis), phenyl carboxylic acids, derivatives of some compounds containing quercetin (e.g. quercetin-7-O-glucoside) and etc.] can naturally reduce metal ions during the nanoparticles production.

A lot of industries such as textile, leather, paper, and plastic produce colored hazardous wastewaters which threaten human health [22, 23]. There are several methods for removing pollutants from wastewaters. Most of them are based on coagulation, freezing, reverse osmosis, active sludge, bacterial function, membrane filtration, ion exchange, oxidation, photocatalytic degradation, ultrafiltration, adsorption, and precipitation and chemical processes [24-26]. The adsorption process (especially with nanoparticles) is a simple and economical technique for treating wastewaters [27].

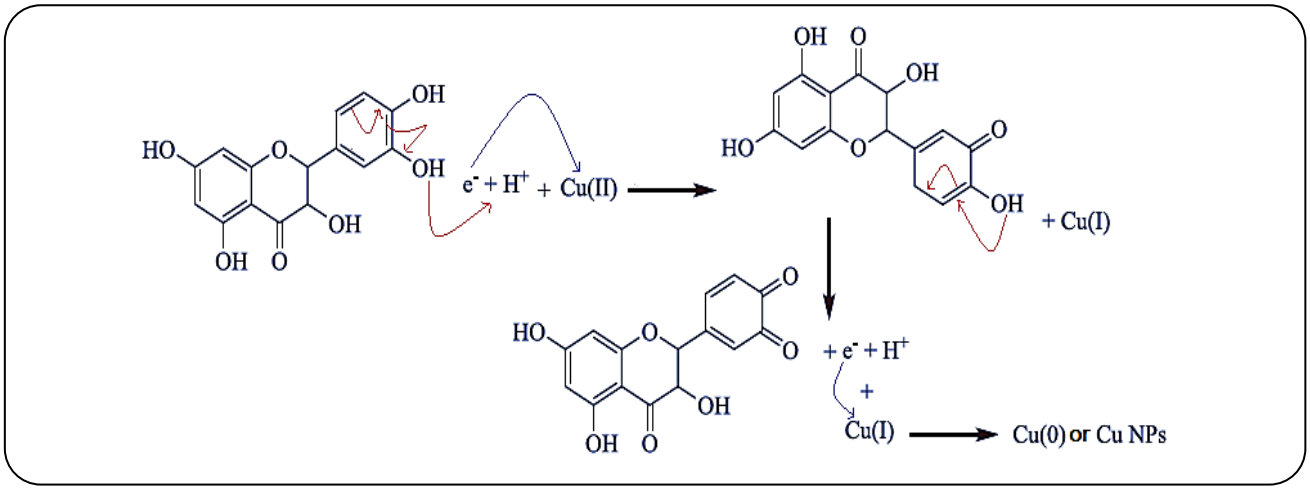

Fig. 2: Schematic of green synthesis of Cu-NPs using quercetin as a polyphenolic compound of Centaurea cyanus plant extract.

Nasrollahzadeh et al. (2019) studied the green synthesis of nanoparticles with various plant extracts for multifunctional applications such as antibacterial and catalytic ones although they (and the other researchers) have never applied it as a dye adsorbent from wastewater [9].

In this reach, Cu-NPs were synthesized by *Centaurea cyanus* plant extract and then characterized by various techniques such as UltraViolet-Visible (UV–Vis) spectroscopy, X-Ray Diffraction (XRD), Fourier Transmission InfraRed (FT-IR) and Transmission Electron Microscopy (TEM). Furthermore, Methylene Blue (MB) as a cationic dye was adsorbed by the synthesized Cu-NPs from an aqueous solution (as the main novelty of this research). This process was initially designed by Design of Experiments (DoE) software. Various parameters such as pH, adsorbent amount (g), MB concentration (mg/L), and time (min) effects were statistically and experimentally considered in this process and optimized. In addition, kinetics and equilibrium isotherms were investigated to understand the MB adsorption by Cu-NPs.

EXPERIMENTAL SECTION

Copper sulfate pentahydrate salt ($CuSO_4.5H_2O$), sodium hydroxide (NaOH), hydrochloric acid (HCl), and methylene blue were purchased from a Merck local supplier.

The *Centaurea cyanus* plants were purchased from a local grocery and washed several times with distilled water. Then, they were dried under ambient conditions and powdered. Five g of this was boiled with 100 mL of distilled water at 70 °C for 50 min. The extraction was mildly carried out under ambient conditions [28]. The extract was passed through Whatman filter paper to remove coarse and suspended particles. The filtered solution was stored in a dark sample jar.

In order to synthesize Cu-NPs, 20 mL of a 0.1 M solution of $CuSO_4.5H_2O$ was transferred to a 100 mL beaker. Then, 20 mL of the extract was dropwise added to 20 mL of the copper sulfate pentahydrate solution.

The color of the solution quickly changed due to copper nanoparticle formation. Then, the nanoparticles were separated from the solution by a laboratory centrifuge (brand: Kaida China, model: TD4K with a maximum speed of 4000 rpm). The nanoparticles were collected and washed with distilled water to remove non-reactive materials. Then, they were dried at ambient temperature.

For the copper nanoparticles formation verification, spectrophotometric (UV-Vis, Shimadzu Japan) analysis and FT-IR (Bruker alpha) were applied. Morphology and size of copper nanoparticles were considered by XRD, FESEM, and TEM devices. In addition, the Zeta Potential (ZP) of Cu-NPs before and after the adsorption process was determined by ZP analyzer (Malvern, UK). Furthermore, the surface properties of synthesized Cu-NPs (surface area, pore-volume, and pore size) were measured by BET/BJH analyzer (Belsorp, Mini II, Japan).

MB solution with a specific concentration was prepared. The initial pH of MB solution was adjusted by NaOH or HCl solutions. According to the experiment's design, the synthetic Cu-NPs (as an adsorbent) were added to the solution. The magnetic stirrer speed was fixed at 200 rpm (without any vortex in the solution). The samples were centrifuged when the time was found. Then,

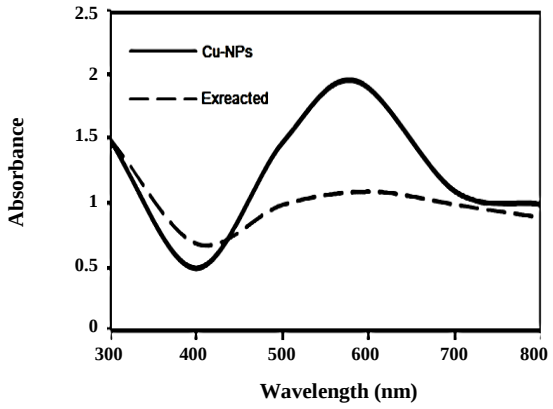

Fig.3: UV-Vis spectrum of Centaurea cyanus plant extract and synthetic Cu-NPs

the samples were analyzed by UV-Vis spectrophotometer in terms of MB concentration. The MB removal was determined by the following equation:

$$MB\ Removal\% = \frac{C_0 - C_t}{C_0} \times 100 \quad (1)$$

where, C_0 and C_t are the initial and time-dependent concentrations, respectively.

In this study, four independent variables including pH (2-11), MB initial concentrations of (5- 200) mg/L, adsorbent amount of (0.01-0.2) g, and contact time of (10-130) min were introduced to the DoE software [29]. Thirty experiments were designed by Design-Expert software (version: 11.0.3 Trial, Stat-Ease Inc., Minneapolis, MN, US) freely downloaded from https://downloadly.ir/software/engineering-specialized/design-expertsite [30]. The mathematical relation between four independent variables and MB removal (response) is shown by the following equation:

$$y = \beta_0 + \sum_{i=1}^{k} \beta_i x_i + \sum_{i=1}^{k} \beta_{ii} x_{ii}^2 + \sum_{1 \le i \le j}^{k} \beta_i x_i + \varepsilon \quad (2)$$

Where β_0 is the constant coefficient. β_i, β_{ii}, and $\beta_{ij}$are the coefficients for the linear, quadratic, and interaction effects, respectively. x_i and x_j are encoded levels for independent variables. k is the number of independent variables and ε is the random error.

RESULTS AND DISCUSSION

Nanoparticles preparation

The *Centaurea cyanus* plant extract was added to the copper sulfate pentahydrate aqueous solution. Copper sulfate pentahydrate solution normally was blue. It changed to green color by adding the extract. Furthermore, it was darker in high concentrations of copper sulfate pentahydrate [4, 5].

Furthermore, UV-Vis spectrophotometric analysis was used to monitor the copper ions reduction to Cu-NPs in the wavelength range of 300-750 nm for investigating maximum adsorption. The maximum desorption was at 560 nm due to surface plasmon resonance which is related to Cu-NPs [31]. Moreover, this peak was not observed in the UV-Vis spectrum pattern prepared by *Centaurea cyanus* plant extract as shown in Fig. 3.

The FT-IR spectrum was also used to find the possible biomolecules which are responsible for capping and stabilizing the Cu-NPs. Fig. 4 shows the FT-IR spectra of Cu-NPs synthesized in the solution. The wavelengths of 3302.65, 2926.42, 2856.45, 1640–1500, and 1114.75 1/cm respectively belong to OH, CH, CH_2, C=O, and COC functional groups, which all confirmed aromatic compounds and derivations of these compounds including polyphenols, terpenoids, proteins and other organic compounds such as carboxylic acids in the *Centaurea cyanus* extract that cover Cu-NPs, which correspond with the earlier reports [32, 33]. Another strong peak is observed within the range of 500–700 1/cm, indicating aromatic compounds of alkanes [34]. The presence of these bands indicates the flavonoids in the stabilization of Cu-NPs. Similar results using the latex of C. *procera* were reported in the literature [35]. This figure also shows the FT-IR spectrum of copper sulfate pentahydrate with strong peaks at 1153.8, 981.199, and 550-600 1/cm, which is characterized by the binding of sulfur to oxygen (S=O) in the $Cu_2SO_4.5H_2O$ salt as a control spectrum [35]. This spectrum only is similar to green synthesized Cu-NPs at 598.1 1/cm. XRD analysis is a very useful and easy tool in identifying the structure of metallic nano-powders [36]. As shown in Fig. 5, the values of 2θ of 43.5°, 50.8°, and 74.6° related to the synthesized Cu-NPs are very close to those of the JCPDS card number 04-0836 [4, 37]. This follows a pure pattern without any contamination at the values of 2θ (because 28.00°, 32.3°, and 36.08° confirm CuO, Cu_2O, and Cu_2O presence, respectively) [38, 39]. The crystallite size of synthesized metallic Cu-NPs in this study was calculated in the range of 10.8-13.3 nm. It indicates that the Cu-NPs size is very small.

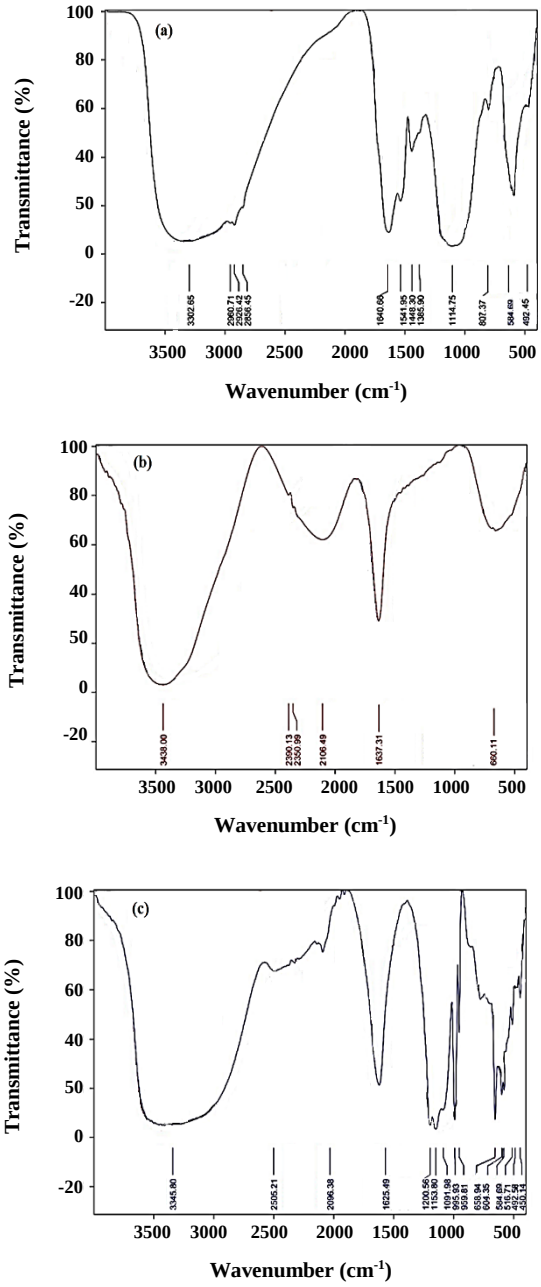

Fig. 4: Fourier-transform infrared spectroscopy analysis (a) synthetic Cu-NPs, (b) Centaurea cyanus plant extract and (c) $Cu_2SO_4.5H_2O$.

The XRD device used in this research was equipped with a chrome lamp. Its outputs were analyzed by High Score software however the other data were measured by the Debye-Scherrer equation [equation (3)].

$$D = \frac{K\,\lambda}{\beta \cos\theta} \qquad (3)$$

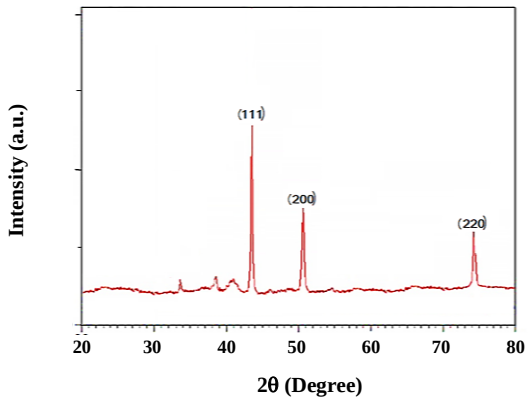

Fig. 5: X-ray powder diffraction pattern of synthetic Cu-NPs.

In this equation, D is the copper crystallite size, λ is the wavelength of the chrome lamp as the X-ray irradiation source 0.229 nm in XRD, K is a Scherrer constant with a value within 0.89, β (radian) is full width at half maximum intensity of diffraction peak and θ (degree) is the Bragg angle, which the values of each in this study f or Cu-NPs are given in Table 1. For example, the average crystallite size of the Cu-NPs for strong and sharp peaks located at 2θ of 43.5 was determined 10.8 nm by the following calculations:

D= 0.89 λ / β Cos θ,

λ= 0.229 nm, 2θ = 43.5 degree, θ = 43.5/2 = 21.75 degree, Cos θ = 0.929 degree

β = 0.01680 radian

D = (0.89) × (0.229 nm)/(0.01680) × (0.929) = 13.05 nm ~ 13.0 nm

Furthermore, the morphology and characteristics of the surface and size of synthetic Cu-NPs were examined by FESEM and TEM [Fig. 6 (a & b)]. According to FESEM analysis, particle size between 9-25 nm was found. The TEM analysis showed that the synthetic nanoparticles were in a spherical shape. According to the literature, the average size of the synthesized nanoparticles was11.9 nm (which agrees with the current research) although bigger nanoparticles than it can be found, as well [40]. This is due to varying the operating conditions such as pH, materials, or/and biomolecules concentration which affect the size of the nanoparticles. In addition, the size distribution was as a histogram inset image [Fig. 6 (b)].

In addition, the results of N_2 adsorption-desorption porosimetry by the Brunauer-Emmett-Teller (BET) analyzer showed that the surface properties of green synthesized

Table 1: XRD analyses of green synthesized Cu-NPs.

Peak	2θ (degree)	β (radian)	hk1(planes)	D (nm)
1	43.5	0.01680	111	13.0
2	50.8	0.02093	200	10.8
3	74.6	0.02018	220	11.3

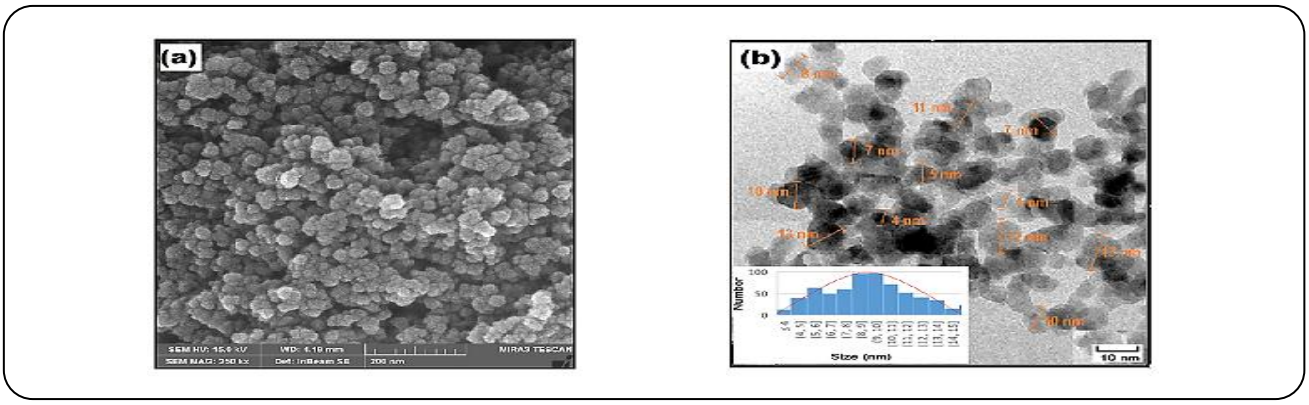

Fig. 6: a) Field Emission Scanning Electron Microscopy image and b) Transmission Electron Microscopy photo of Cu-NPs.

Cu-NPs including mean surface area, mean pore volume, and mean pore size are 74.2 m^2/g, 0.36 cm^3/g, and 19.3 nm, respectively.

Analysis of variance (ANOVA) consideration

According to Table 2, the effects of four independent variables including adsorbent amount (g), pH, MB concentration (mg/L), and time (min) on the MB removal were considered. Analysis of variance (ANOVA) statistically shows significant variables and the effects of their interactions on the response. According to this analysis, F and P values use to evaluate the suggested model. If the F-value for a fitted model is a high amount and the P-value is less than 0.05, the proposed model will be acceptable [41]. According to the approximation of "lack-of-fit" a modified quadratic expression can properly show a relationship between the variables [Eq. (4)]:

$$\text{MB removal\%} = -2.16183+336.90398A-0.856843B+0.452638C-0.269633D+6.62005AD-2.00980AD-0.002376C^2+0.001524D^2 \quad (4)$$

Where, *A*, *B*, *C*, and *D* are adsorption amount (g), pH, time (min), and MB initial concentration (mg/L), respectively.

According to the ANOVA (Table 3), most of the factors are significant except pH, interactions of adsorbent amount with pH, adsorbent amount with time, pH with time, the square of adsorbent amount, and pH which are ignorable. The statistical criteria of the modified model showed a value of 0.966 for the coefficient of determination. It implies that 96.6 % of data variations were considered. Adj-R^2 value (0.934) was very close to the corresponding R^2 value. Moreover, Pred-R^2 (0.821) was in reasonable agreement with the Adj-R^2. The F and P values respectively were at 30.30 and 0.0001 which implies that the model is a satisfactory one. Furthermore, the lack-of-fit (3.57) implies that it does not significantly depend on the Pure Error.

The zeta potential of Cu-NPs was measured in the experimental pH range of 2-11 before the adsorption process. It was found that surface charge is positive at low pHs (ZP value was around 17 mV) and remains constant at higher pHs. Its reason is due to the electrostatic interactions between negative charges of adsorbent and positive charges of MB dye. It was also observed that ZP value did not significantly change after the adsorption process and remained almost constant. Since the ZP was at 17 mV and remained constant over a period, it confirmed the stability of Cu-NPs. This is due to being biomolecules (as a stabilizing agent) in the extract. Furthermore, the ZP shows the surface charge of particles. The surface charge of particles increases when the ZP increases. In fact,

Table 2: Independent variables and their response on methylene blue removal percentage.

Run	Adsorbent amount (g)	pH	Time (min)	MB concentration (mg/L)	Removal%	
					Observed	Predicted
1	0.057	9.5	40	53.75	4.60	7.09
2	0.153	4.5	100	53.75	58.95	57.19
3	0.105	7	70	200.00	19.51	22.70
4	0.057	9.5	40	151.25	7.40	9.98
5	0.105	7	70	102.50	21.65	22.08
6	0.153	4.5	100	151.25	28.70	26.10
7	0.057	9.5	100	53.75	9.51	12.50
8	0.105	2	70	102.50	20.24	21.73
9	0.105	7	70	102.50	23.45	22.05
10	0.105	7	130	102.50	23.70	19.76
11	0.153	9.5	100	151.25	27.54	29.30
12	0.105	7	70	102.50	18.31	22.07
13	0.200	7	70	102.50	45.01	48.62
14	0.105	7	10	102.50	4.73	8.02
15	0.153	9.5	40	151.25	28.70	24.80
16	0.057	4.5	40	151.25	10.84	7.69
17	0.153	4.5	40	151.25	22.00	19.84
18	0.153	4.5	40	53.75	41.21	42.67
19	0.105	7	70	5.00	55.06	51.09
20	0.105	7	70	102.50	22.60	22.07
21	0.057	4.5	40	53.75	14.72	11.09
22	0.057	4.5	100	151.25	3.60	6.68
23	0.057	4.5	100	53.75	15.50	19.20
24	0.153	9.5	40	53.75	42.76	40.43
25	0.153	9.5	100	53.75	50.21	53.17
26	0.105	7	70	102.50	23.48	22.07
27	0.010	7	70	102.50	0.36	0.02
28	0.105	7	70	102.50	25.48	22.07
29	0.105	12	70	102.50	22.12	20.02
30	0.057	9.5	100	151.25	8.86	7.21

Table 3: Analysis of variance for the response quadratic model.

Source	Sum of squares	Degree of freedom	Mean squares	F-value	P-value	
Model	6619.51	14	472.82	30.30	< 0.0001	significant
A-ad	4116.37	1	4116.37	263.76	< 0.0001	
B-pH	6.23	1	6.23	0.3991	0.5371	
C-time	195.77	1	195.77	12.54	0.0030	
D-con	1114.08	1	1114.08	77.79	< 0.0001	
AC	59.52	1	59.52	3.81	0.0478	
AD	328.89	1	328.89	21.07	0.0004	
C^2	125.43	1	125.43	8.04	0.0125	
D^2	359.6	1	359.6	23.04	0.0002	
Residual	234.10	15	15.61			
Lack of Fit	205.33	10	20.53	3.57	0.0847	not significant
Pure Error	28.77	5	5.75			
Cor. Total	6853.61	29				

R^2 = 0.966, Adj-R^2 = 0.934, Pred-R^2= 0.821

the ZP influences the particle stability in suspension through the electrostatic repulsion between particles.

Process optimization

The optimum conditions for the predicted data were found using DoE software. The process optimization was performed based on the desirability function [41, 42]. The main objective of this study was to maximize the MB removal by recalculating all responsible factors by the desirability function. Table 2 lists some parameters used for the optimization process. The upper and lower limits of all parameters and the model response were obtained from the CCD levels. Therefore, the software predicted 66.58%. of MB removal for the optimized conditions as adsorbent amount of 0.15(g), MB initial concentration of 30 (mg/L), pH of 6.6, and time of 101.5 (min). These conditions were experimentally prepared and the MB removal percentage was experimentally obtained at 63.20%. However some conditions such as the adsorbent amount of 0.15 (g), MB initial concentration of 53.75 (mg/L), pH of 4.5, and time of 100 (min) (Table 2, second row) were reported for 55% of the predicted and 53% of observed MB removal percentage but, they cannot be as optimum conditions because the variables effects and their interactions have not carefully been considered.

Adsorption kinetics

Several kinetic models were applied to examine the experimental data to find which process stage can control the process [43-45]. For this purpose, three kinetic models including pseudo-first-order, pseudo-second-order, and intramolecular diffusion were applied. As shown in Table 4, all necessary equations were extracted from literature and calculated data were then illustrated [46, 47]. The pseudo-second-order kinetic model could properly legitimize (with a high R^2) this process. This confirms that the rate-limiting step in this process is the chemical interactions between Cu-NPs surface and MB molecules (chemisorption).

Fig. 7 shows the experimental and predicted data using various kinetic models at ambient temperature and MB initial concentration of 30 mg/L. As shown in this figure, all data were properly predicted by the pseudo-second-order model.

Adsorption isotherms

The equilibrium data were examined using several isotherm models such as Langmuir, Freundlich, and Temkin ones. In fact, adsorption isotherm is studied by shaking solutions with various MB initial concentrations (5-200 mg/L) at optimum conditions. As shown in Table 5,

Table 4: Various kinetic models and their data for MB adsorption (pH of 6.6, Cu-NPs amount of 0.15 g and time of 101.5 min).

Model	Parameters	MB Concentration (mg/L)		
		10	20	30
Pseudo-first order kinetic $\log(q_e-q_t) = \log(q_e) - k_1t/2.303$	k_1 (1/min)	0.029	0.032	0.327
	q_e (calc.): (mg/g)	9.475	14.488	21.014
	R^2	0.895	0.898	0.904
Pseudo-second order kinetic $(t/q_t) = 1/(k_2q_e^2) + t/q_e$	k_2 (g/mg) (1/min)	0.248	0.360	0.359
	q_e (calc.): (mg/g)	12.446	25.060	36.230
	R^2	0.989	0.996	0.996
Intramolecular diffusion $q_t = K_{dif}\, t^{1/2} + C$	K_{diff} (mg/g 1/min$^{1/2}$)	0.848	2.362	3.411
	C (mg/g)	-1.596	5.583	8.023
	R^2	0.837	0.786	0.788

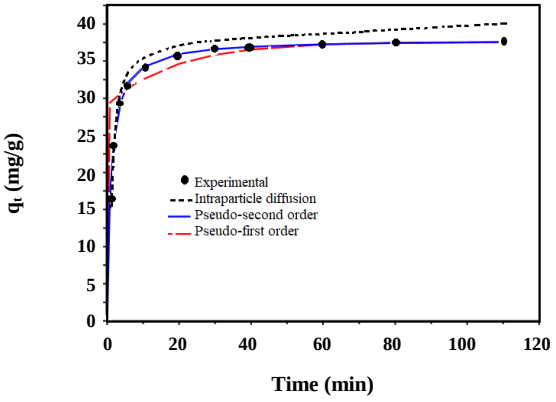

Fig. 7: Various kinetic models for the adsorption of MB onto Cu-NPs under the optimum condition: pH of 6.6, Cu-NPs amount of 0.15 g, and MB initial concentration of 30 mg/L.

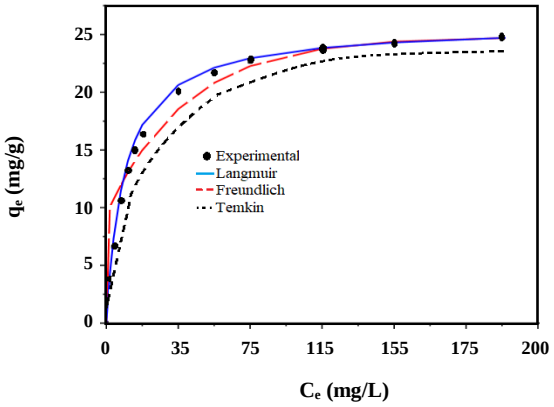

Fig. 8: The equilibrium adsorption isotherms for adsorption of MB using Cu-NPs under optimum conditions: pH of 6.6, Cu-NPs amount of 0.15 g, and time of 101.5 min.

all equations in linear forms were extracted from the literature and calculated data were then illustrated [48, 49]. According to R^2 values, necessary Langmuir, Freundlich, and Temkin isotherm models could respectively be fitted on the data. This confirms that the MB adsorption process on Cu-NPs is a monolayer one. In fact, The Langmuir model with a maximum adsorption capacity of 21.9 mg/g using Cu-NPs (0.15 g) can fantastically legitimize this process although, the Freundlich model can eligibility legitimize it, as well. The experimental data and corresponding calculated ones by various adsorption models are shown in Fig. 8.

Comparison with the other studies

According to the literature, a good removal was obtained through the adsorption process by Cu-NPs at the optimum conditions because some references with the other adsorbents reported 10.55%, 9.81%, 10.82%, 30.70%, and 34.50% for MB removal, respectively [50, 51]. Furthermore, a reference only reported 71.43% for MB removal [52]. It is concluded that the activated carbon from the sludge of the food processing industry under a controlled pyrolysis process with $ZnCl_2$ as an activating agent can only remove MB more than that of the current research. Also, the performance of green synthesized Cu-NPs was compared with the other adsorbents as summarized in Table 6. As shown in this table, the middle adsorption of MB on Cu-NPs can be carried out by green and economic technique for nanoparticle preparation as illustrated in this research.

Table 5: Various isotherm models equations for MB adsorption and their parameters: pH of 6.6, MB concentration rang of 5-200 mg/g and time of 101.5 min.

Isotherm	Parameters	Cu-NPs amount (g)	
		0.15	0.2
Langmuir $1/q_e= 1/(K_aQ_m C_e)+1/Q_m$	Q_m (mg/g) K_a (L/mg) R^2 R_L	21.860 0.013 0.999 0.433-0.792	27.397 0.009 0.996 0.514-0.841
Freundlich $q_e = \ln K_F + (1/n) \ln C_e$	n K_F (mg/g) (L/mg)$^{1/n}$ R^2	1.387 0.494 0.995	1.304 0.429 0.986
Temkin $q_e=(RT/b_T)\ln(AC_e)$	A (1/g) b_T(J/mol) R^2	0.201 523.759 0.9880	0.168 613.448 0.9930

Table 6: MB removal Comparison by various adsorbents.

Adsorbent	Size(nm)	Shape	Operating conditions	Q_m(mg/g)	RE(%)	Ref.
Biochar/iron oxide	29	Amorphous	pH=6.1 [MB)]=50 mg/L [adsorbent]=10 mg/L t=12 h T=: 293 K	862.0	95.1	[53]
Cu-NPs	14.2	Spherical	pH=6 [MB)]=25 mg/L [adsorbent]=25 mg/L t=80 min T= 295 K	64.0	34.0	[54]
ZnONPs-PWAC	22-35	Spherical	pH= 10 [MB]=20 mg/L [adsorbent]=50mg/L t=3 h T= -	-	99.0	[55]
Fe_3O_4@ABDA	12	Spherical	pH= 7 [MB)]=150 mg/L [adsorbent]=50 mg/L t=180 min T=298 K	123.5	92.5	[56]
Si/Cu	8	Amorphous	pH= 8 [MB)]=90 mg/L [adsorbent]=750 mg/L t=60 min T:298 k	82.3	93.8	[57]
Magnetized *Tectonagrandis* sawdust	-	-	pH= 8 [MB)]=100 mg/L [adsorbent]=1000 mg/L t=60 min T=308 K	172.4	90.8	[58]
CS-MgONP			pH= 7.3 [MB)]=19.4 mg/L [adsorbent]=470 mg/L t=60 min T=310 K	163.9	94.5	[59]
Cu-NPs	11.9	Spherical	pH= 6.6 [MB)]=30 mg/L [adsorbent]=150 mg/L t= 101.5 min T=298 K	21.9	63.2	Current study

CONCLUSIONS

In the study, Cu-NPs were prepared with a green and economic technique. The nanoparticles were spherical and had an average crystallite size of ~11.9 nm. The ZP, mean surface area and pore volume of the prepared nanoparticles were determined as 17 mV, 74.2 m^2/g, and 0.36 cm^3/g, respectively. CCD was applied to study four independent variables (such as pH, adsorption amount, time, and MB initial concentration) effects on MB removal. A quadratic expression with R^2 value of 0.966 was found to show a relationship between the variables. The results of (ANOVA) analysis indicated that adsorbent amounts can dramatically increase MB removal compared with the other variables. The MB removal of 63.20 % was obtained at pH of 6.6, MB initial concentration of 30mg/L, Cu-NPs amount of 0.15 g, and time of 101.5 min as optimum conditions. Furthermore, a pseudo-second-order model with a rate constant of 0.359 (g/mg) (1/min) could properly model this process kinetics under the optimum condition. Moreover, the Langmuir equation with a maximum adsorption capacity of 21.9 mg/g was isothermally able to model this process, as well.

Acknowledgments

Our real debt of gratitude goes to Arak University for this work financial support (Grant N

Received: Jun. 25, 2020; Accepted: Sep. 14, 2020

REFERENCES

[1] Sreeju N., Rufus A., Philip D., Microwave-Assisted Rapid Synthesis of Copper Nanoparticles with Exceptional Stability and their Multifaceted Applications, *J. Mol. Liq.*, **221**: 1008–1021 (2016).

[2] Kumar R.V., Mastai Y., Diamant Y., Gedanken A., Sonochemical Synthesis of Amorphous Cu and Nanocrystalline CuO Embedded in a Polyaniline Matrix, *J. Mater. Chem.*, **11(4)**: 1209–1213 (2001).

[3] Lisiecki I., Pileni M.P., Synthesis of Copper Metallic Clusters Using Reverse Micelles as Microreactors, *J. Am. Chem. Soc.*, **115(10)**: 3887–3896 (1993).

[4] Suárez-Cerda J., Espinoza-Gómez H., Alonso-Núñez G.,Rivero I.A.,Gochi-Ponce Y., Flores-López L.Z., A Green Synthesis of Copper Nanoparticles Using Native Cyclodextrins as Stabilizing Agents, *J. Saudi Chem. Soc*., **21(3)**: 341–348 (2017).

[5] Nasrollahzadeh M., Sajadi S.M., Khalaj M., Green Synthesis of Copper Nanoparticles Using Aqueous Extract of the Leaves of Euphorbia Esula L and Their Catalytic Activity for Ligand-Free Ullmann-Coupling Reaction and Reduction of 4-Nitrophenol, *RSC Adv*., **4(88)**: 47313–47318 (2014).

[6] Varshney R., Bhadauria S., Gaur M.S., Pasricha R., Characterization of Copper Nanoparticles Synthesized by a Novel Microbiological Method, *JOM*, **62(12)**: 102–104 (2010).

[7] Kolekar R., Bhade S., Kumar R., Reddy P., Singh R., Biosynthesis of Copper Nanoparticles Using Aqueous Extract of Eucalyptus Sp. Plant Leaves, *Curr. Sci.*, **109(2)**: 255–257 (2015).

[8] Heera P., Shanmugam S., Ramachandran, Green Synthesis of Copper Nanoparticle Using Gymnema sylvestre by Different Solvent Extract, *Int. J. Curr. Res.*, **3(12)**: 268–275 (2015).

[9] Nasrollahzadeh M., Atarod M., Sajjadi M., Sajadi S.M., Issaabadi Z., Plant-Mediated Green Synthesis of Nanostructures: Mechanisms, Characterization, and Applications, *Interface Sci. Technol.*, **28**: 199–322 (2019).

[10] Si S., Mandal T.K., Tryptophan-Based Peptides to Synthesize Gold and Silver Nanoparticles: A Mechanistic and Kinetic Study, *Chem. A. Eur. J.*, **13(11)**: 3160–3168 (2007).

[11] Kim J., Rheem Y., Yoo B., Chong Y., Bozhilov K.N., Kim D., Sadowsky M.J., Hur H.G., Myung N.V., Peptide-Mediated Shape- and Size-Tunable Synthesis of Gold Nanostructures, *Acta Biomater*.,**6(7)**: 2681–2689 (2010).

[12] Nasrollahzadeh M., Sajadi S.M., Preparation of Au Nanoparticles by Anthemisxylopoda Flowers Aqueous Extract and their Application for Alkyne/Aldehyde/Amine A3-Type Coupling Reactions, *RSC Adv.*, **5(57)**: 46240–46246 (2015).

[13] Nasrollahzadeh M., Sajadi S.M., Maham M., Tamarixgallica Leaf Extract Mediated Novel Route for Green Synthesis of CuO Nanoparticles and Their Application for N-Arylation of Nitrogen-Containing Heterocycles Under Ligand-Free Conditions, *RSC Adv*., **5(51)**: 40628–40635 (2015).

[14] Rafique M., Shaikh A.J., Rasheed R., Tahir M.B., Bakhat H.F., Rafique M.S., Rabbani F., A Review on Synthesis, Characterization and Applications of Copper Nanoparticles Using Green Method, *Nano*., **12(4)**: 1750043 (2017).

[15] Ebrahiminezhad A., Zare-Hoseinabadi A., Sarmah A.K., Taghizadeh S., Ghasemi Y., Plant-Mediated Synthesis and Applications of Iron Nanoparticles, *Mol. Biotechnol*., **60(2)**: 154–168 (2018).

[16] Nayak D., Pradhan S., Ashe S., Rauta P.R., Nayak B., Biologically Synthesized Silver Nanoparticles from Three Diverse Family of Plant Extracts and their Anticancer Activity Against Epidermoid A431 Carcinoma, *J. Colloid Interface Sci*., **457**: 329–338 (2015).

[17] Nasrollahzadeh M., Sajadi S.M., Green Synthesis of Copper Nanoparticles Using Ginkgo Biloba L. Leaf Extract and Their Catalytic Activity for the Huisgen[3+ 2] Cycloaddition of Azides and Alkynes at Room Temperature, *J. Colloid Interface Sci*., **457**: 141–147 (2015).

[18] Gorobets O., Gorobets S., Koralewski M., Physiological Origin of Biogenic Magnetic Nanoparticles in Health and Disease: from Bacteria to Humans, *Int. J. Nanomedicine*., **12**: 4371–4395 (2017).

[19] Shamaila S., Sajjad A.K.L., Ryma N.A., Farooqi S.A., Jabeen N., Majeed S., Advancements in Nanoparticle Fabrication by Hazard Free Eco-Friendly Green Routes, *Appl. Mater. Today*, **5**: 150–199 (2016).

[20] Pirvu L., Dragomir C., Schiopu S., Mihul S.C., Vegetal Extracts with Gas Troprotective Activity. Part. I. Extracts Obtained from *Centaureacyanus*L. Raw Material, *Rom. Biotechnol. Lett.*, **17(2)**: 7169–7176 (2012).

[21] Kuś P.M., Jerković I., Tuberoso C.I.G., Marijanović Z., Congiu F., Cornflower (Centaurea Cyanus L.) Honey Quality Parameters: Chromatographic Fingerprints, Chemical Biomarkers, Antioxidant Capacity, and Others, *Food Chem*., **142**: 12–18 (2014).

[22] Yang S.T., Chen S., Chang Y., Cao A., Liu Y., Wang H., Removal of Methylene Blue from Aqueous Solution by Graphene Oxide, *J. Colloid Interface Sci.*, **359(1)**: 24–29 (2011).

[23] Li W.H., Yue Q.Y., Gao B.Y., Ma Z.H., Li Y.J., Zhao H.X., Preparation and Utilization of Sludge-Based Activated Carbon for the Adsorption of Dyes from Aqueous Solutions, *Chem. Eng. J.*, **171(1)**: 320–327 (2011).

[24] Hao O.J., Kim H., Chiang P.C., Decolorizationof Wastewater, Crit. Rev., *Env. Sci. Tech.*, **30(4)**: 449–505 (2000).

[25] Aksu Z., Application of Biosorption for the Removal of Organic Pollutants: A Review, *Process Biochem*., **40(3-4)**: 997–1026 (2005).

[26] Gupta V.K., Application of Low-Cost Adsorbents for Dye Removal – A Review, *J. Environ. Manag*., **90(8)**: 2313–2342 (2009).

[27] Asgher M., Bhatti H.N., Evaluation of Thermodynamics and Effect of Chemical Treatments on Sorption Potential of Citrus Waste Biomass for Removal of Anionic Dyes from Aqueous Solutions, *Ecol. Eng.* **38(1)**: 79–85 (2012).

[28] Asadi S., Green Synthesis of Cu-NPs Using *Centaurea cyanus* Plant Extract and their Application in the Adsorption Process, MSc. Thesis, Arak University, Iran (2019).

[29] Davarnejad R., Pishdad R., Sepahvand S., Dye Adsorption on the Blends of Saffron Petals Powder with Activated Carbon: Response Surface Methodology, *Inter. J. Eng. Trans. C: Aspects*, **31**: 2001–2008 (2018).

[30] Montgomery D.C., "Design and Analysis of Experiments", 5th ed., John Wiley & Sons, Inc., New York, (2001).

[31] Chung I., Abdul Rahuman A., Marimuthu S., Kirthi A., Anbarasan K., Padmini P., Rajakumar G., Green Synthesis of Copper Nanoparticles Using Ecliptaprostrata Leaves Extract and Their Antioxidant and Cytotoxic Activities, *Exp. Ther. Med*., **14(1)**: 18–24 (2017).

[32] Ramesh M., Anbuvannan M., Viruthagiri G., Green Synthesis of ZnO Nanoparticles Using Solanumnigrum Leaf Extract and Their Antibacterial Activity, *Spectrochim. Acta Part A: Molec. Biomolec. Spectrosc*.,**136**: (Part B) 864–870 (2015).

[33] Grasel F.d.S., Ferrão M.F., Wolf C.R., Development of Methodology for Identification the Nature of the Polyphenolic Extracts by FT-IR Associated with Multivariate Analysis, *Spectrochim. Acta Part A Mol. Biomol. Spectrosc.*, **153**: 94–101 (2016).

[34] Harne S., Sharma A., Dhaygude M., Joglekar S., Kodam K., Hudlikar M., Novel Route for Rapid Biosynthesis of Copper Nanoparticles Using Aqueous Extract of Calotropisprocera L. Latex and Their Cytotoxicity on Tumor Cells, *Colloids Surf. B Biointerfaces*, **95**: 284–288 (2012).

[35] Oger N., Lin Y.F., Labrugère C., Le Grognec E., Rataboul F., Felpin F.X., Practical and Scalable Synthesis of Sulfonatedgraphene, *Carbon*, **96**: 342–350 (2016).

[36] Mourdikoudis S., Pallares R.M., Thanh N.T.K., Characterization Techniques for Nanoparticles: Comparison and Complementarity upon Studying Nanoparticle Properties, *Nanoscale*, **10**: 12871–12934 (2018).

[37] MDI (Material Data) Jade Software, Version 6.5, XRD Data Processing Card ≠040-836

[38] Alekseeva O., Chulovskaya S., Bagrovskaya N., Parfenyuk V., Copper Nanoparticle Composites Based on Cellulose Derivatives, *Chem. Chem. Technol*., **5** (4):447–450 (2011).

[39] Sadanand V., Rajini N., Varada A., Satyanarayana B., Preparation of Cellulose Composites with *in Situ* Generated Copper Nanoparticles Using Leaf Extract and their Properties, *Carbohydr Polym.*, **150**: 32–39 (2016).

[40] Khatami M., Heli H., Mohammadzadeh Jahani P., Azizi H., Lima Nobre M.A., Copper/Copper Oxide Nanoparticles Synthesis using Stachys Lavandulifolia and its Antibacterial Activity, *IET Nanobiotechnol*, **11(6)**: 709–371 (2017).

[41] Sakkas V.A., Islam M., Stalikas C., AlbanisT.A., Photocatalytic Degradation Using Design of Experiments: A Review and Example of the Congo Red Degradation, *J. Hazard. Mater*., **175(1-3)**: 33–34 (2010).

[42] Ali N., Teixeira J.A., Addali A., A Review on Nanofluids: Fabrication, Stability, and the Rmophysical Properties, *J. Nanomaterials*. **2018**: 1–33 (2018).

[43] Lagergren S., Sven K., Citation Review of Lagergren Kinetic Rate Equation on Adsorption Reactions, *Handl*, **24(4)**: 1–39 (1898).

[44] Ho Y.S., McKay G., Kinetic Models for the Sorption of Dye from Aqueous Solution by Wood, *Proc. Safty. Environ. Protect*.,**76(2)**: 183–191 (1998).

[45] Wu F.C., Tseng R.L., Juang R.S., Kinetic Modeling of Liquid-Phase Adsorption of Reactive Dyes and Metal Ions on Chitosan, *Water Res*., **35(3)**: 613–618 (2001).

[46] Ho Y.S., McKay G., Pseudo-Second Order Model for Sorption Processes, *Process Biochemi*., **34(5)**: 451–465 (1999).

[47] Weber W.J., Morris J.C., Kinetics of Adsorption on Carbon from Solution, *J. Sanitary Eng. Division*, **89(2)**: 31–60(1963).

[48] Freundlich H., ÜberDie Adsorption in Lösungen, *Zeitschrift für physikalische, Chemie*, **57(28)**: 385–470 (1907).

[49] Temkin M.I., Pyzhev V., Kinetics of Ammonia Synthesis on Promoted Iron Catalyst, *Acta Physicochimica. URSS*, **12**: 217–222 (1940).

[50] Han R., Wang Y., Han P., Shi J., Yang J., Lu Y., Removal of Methylene Blue from Aqueous Solution by Chaff in Batch Mode, *J. Hazard. Mater.*, **137(1)**: 550–557 (2006).

[51] Ghaedi M., Heidarpour S., NasiriKokhdan S., Sahraie R., Daneshfar A., Brazesh B., Comparison of Silver and Palladium Nanoparticles Loaded on Activated Carbon for Efficient Removal of Methylene Blue: Kinetic and Isotherm Study of Removal Process, *Powder Technol.*, **228**: 18–25 (2012).

[52] Mahapatra K., Ramteke D.S., Paliwal L.J., Production of Activated Carbon from Sludge of Food Processing Industry under Controlled Pyrolysis and its Application for Methylene Blue Removal, *J. Anal. Appl. Pyrol.*, **95**: 79–86 (2012).

[53] Zhang P., Connor D., Wang Y., Jiang L., Xia T., Wang L., Tsang D., Sikok Y., Hou D., A Green Biochar/Iron oxide Composite for Methylene Blue Removal, *J. Hazard. Mater.*, **384**: 121286 (2020).

[54] Sebei N., Jabli M., Ghith A., Saleh T.A., Eco-friendly Synthesis of Cynomorium Coccineum Extract for Controlled Production of Copper Nanoparticles for Sorption of Methylene Blue Dye, *Arabian. J. Chem.*, **13(2)**: 4263–4274 (2020).

[55] Kamaraj M., Srinivasan N.R., Assefa G., Adugna A.T., Kebede M., Facile Development of Sunlit ZnO Nanoparticles-Activated Carbon Hybrid from Pernicious Weed as an Operative Nano-Adsorbent for Removal of Methylene Blue and Chromium from Aqueous Solution: Extended Application in Tannery Industrial Wastewater, *Environ. Technol.Inno*., **17**: 100540 (2020).

[56] Aldawsari A.M., Fe_3O_4@ABDA Nanocomposite as a New Adsorbent Effective Removal of Methylene Blue Dye: Isotherm, Kinetic, and Thermodynamic Study, Sep. Sci. Technol., 1-11 (2020).

[57] Hameed A.M., Synthesis of Si/Cu Amorphous Adsorbent for Efficient Removal of Methylene Blue Dye from Aqueous Media, *J. Inorg. Organomet. Polym.*, **30:** .2881-2889 (2020)

[58] Mashkoor F., Nasar A., Magnetized Tectona Grandis Sawdust as a Novel Adsorbent: Preparation, Characterization, and Utilization for the Removal of Methylene Blue from Aqueous Solution, *Cellulose*, **27**: 2613–2635 (2020).

[59] Myneni V.R., Rao Kanidarapu N., Vangalapati M., Methylene Blue Adsorption by Magnesium Oxide Nanoparticles Immobilized with Chitosan (CS-MgONP): Response Surface Methodology, Isotherm, Kinetics and Thermodynamic Studies, *Iran. J. Chem. Chem. Eng. (IJCCE)*, **39(6):** 29-42 (2020).